



HAL
open science

A Study of a Large Bipolar Lightning Event Observed at the Säntis Tower

Mohammad Azadifar, Marcos Rubinstein, Farhad Rachidi, Vladimir Rakov, Gerhard Diendorfer, Wolfgang Schulz, Davide Pavanello

► **To cite this version:**

Mohammad Azadifar, Marcos Rubinstein, Farhad Rachidi, Vladimir Rakov, Gerhard Diendorfer, et al.. A Study of a Large Bipolar Lightning Event Observed at the Säntis Tower. *IEEE Transactions on Electromagnetic Compatibility*, 2019, 61 (3), pp.796-806. 10.1109/TEMC.2019.2913220 . hal-03589921

HAL Id: hal-03589921

<https://hal.science/hal-03589921v1>

Submitted on 26 Feb 2022

HAL is a multi-disciplinary open access archive for the deposit and dissemination of scientific research documents, whether they are published or not. The documents may come from teaching and research institutions in France or abroad, or from public or private research centers.

L'archive ouverte pluridisciplinaire **HAL**, est destinée au dépôt et à la diffusion de documents scientifiques de niveau recherche, publiés ou non, émanant des établissements d'enseignement et de recherche français ou étrangers, des laboratoires publics ou privés.

A Study of a Large Bipolar Lightning Event Observed at the Säntis Tower

Mohammad Azadifar, Marcos Rubinstein, Fellow, IEEE, Farhad Rachidi, Fellow, IEEE, Vladimir A. Rakov, Fellow, IEEE, Gerhard Diendorfer, IEEE, Wolfgang Schulz, Davide Pavanello

Abstract— An unusual negative lightning flash was recorded at the Säntis Tower on June 15, 2012. The flash did not contain an initial continuous current typical of upward negative lightning, which is the most common type of event at the Säntis Tower. The flash contained 4 strokes, the last 3 of which were normal while, the current associated with the first stroke resembled a Gaussian pulse with an unusually high peak value of 102.3 kA, a long risetime of 28.4 μ s, and a pulse width of 53.8 μ s, which was followed by an opposite polarity overshoot with a peak value of 8.5 kA. Our current records suggest the involvement of a long upward connecting positive leader in response to the approaching downward negative leader in the formation of this flash. LLS data indicate that a positive cloud-to-ground stroke occurred 1 ms prior to the first stroke of the flash.

In this paper, we present a detailed description of the data associated with this event. Moreover, both a return stroke model and an M-component model are used to reproduce the far-field waveform of this bipolar stroke. The simulations result in a radiated electric field waveform that is similar to those of Large Bipolar Events (LBEs) observed in winter thunderstorms in Japan. A sensitivity analysis of the used simulation models reveals that, by proper selection of the input parameters, all field waveform characteristics, except for the positive half-cycle width, can be made to fall in the range of LBE field characteristics reported in Japan.

Index Terms— Lightning Charge Transfer Mode, Downward Negative Leader, Numerical Modeling, Large Bipolar Event.

I. INTRODUCTION

High-current lightning discharges are reported to be one of the main features of winter lightning in Japan [1].

Mohammad Azadifar and Marcos Rubinstein are with the IICT institute of Heig-vd, Yverdon-les-Bains, Switzerland. is with the University of Applied Sciences Western Switzerland, Yverdon-les-Bains 1400, Switzerland (e-mail: mohammad.azadifar@heig-vd.ch, marcos.rubinstein@heig-vd.ch).

Gerhard Diendorfer and Wolfgang Schulz are with OVE Service GmbH, Dept. ALDIS, Vienna, Austria (email: G.Deindorfer@ove.at, W.Schulz@ove.at).

Farhad Rachidi and Mario Paolone are with the Swiss Federal Institute of Technology, Lausanne 1015, Switzerland (email: farhad.rachidi@epfl.ch, mario.paolone@epfl.ch).

Davide Pavanello is with the University of Applied Sciences of Western Switzerland, Sion CH-1950, Switzerland (e-mail: davide.pavanello@hevs.ch). Vladimir Rakov is with the Department of Electrical and Computer Engineering, University of Florida, Gainesville, FL 32611 USA, and also with the Institute of Electronics and Mathematics, Natural Research University, Higher school of Economics, Russia (e-mail: rakov@ece.ufl.edu).

They constitute one of the major causes for transmission line outages [2]. These high-current lightning discharges are known to have bipolar field signatures which makes them different from usual return strokes. They are known as Large Bipolar Events (LBEs) and they are related to cloud-to-ground discharges, as suggested by slow field antenna records that show that they are associated with charge transfer to the ground [2]. Both positive and negative initial polarities of electric fields from LBEs have been reported. The observed bipolar pulses associated with LBEs are clearly different from the characteristic field waveforms of first return strokes in downward lightning, since the latter exhibit a slow-front/fast-transition in their rising portion preceded by small unipolar pulses associated with the downward stepped leader [3].

Due to the high occurrence of LBEs during the winter period, it is believed that the height of the cloud charge centers must be lower compared to the one characterizing normal return strokes. This fact has been confirmed using the reported height of the -10 degree isotherm [4]. An inverted return stroke model, called “GC (Ground-to-Cloud) stroke model” involving a long upward leader was proposed by Ishii and Saito [2] to simulate the bipolar field signature of these events. Using the “inverted” return stroke model and the channel-base current waveform, Saito and Ishii [5] reproduced electric fields of LBEs observed at 117 km. Using the transmission line (TL) model, Kaneko et al. [6] also reproduced the bipolar magnetic field signatures of LBEs measured at distances of 12.6 to 129.6 km.

Using numerical simulations based on the bouncing wave model (developed by Nag and Rakov [7] for Compact Intracloud Discharges or CIDs), Chen et al. [8] suggested that the only current waveform that can reproduce the field signature of LBEs is a symmetrical Gaussian pulse.

An extensive study on the bipolar field signatures of high current discharges (Large Bipolar Events) was presented by Wu et al. [9]. The electric field signature of LBEs reported by Wu et al. is characterized by a bipolar, symmetrical pulse whose initial polarity is the same as that of negative return strokes. The waveforms presented by Wu et al. were all located inland, and 74 % of them were isolated in time. Wu et al. pointed out some similarities between LBEs and NBEs (Narrow Bipolar Events, which is just another name for CIDs): both produce a bipolar electric field, both are associated with a very large current, both are of short duration and they possibly happen in a short channel length. They also suggested that LBEs and NBEs appear during winter and summer thunderstorms, respectively. They further stated that LBEs are probably associated with high grounded

objects and they hypothesized that LBEs occur when the negative charge layer in thunderclouds is close to the top of the tall, grounded object since this would explain why LBEs were observed predominantly during winter time.

An overview of LBEs and other similar events is given by Zhu et al. [10]. The reviewed data were obtained both in winter and in summer, but in all cases a tall strike object was involved. Zhu et al. [11] presented a modeling study of LBE-like events.

Even though all of these studies suggest that LBEs are due to a cloud-to-ground discharge process with channel lengths shorter than those of return strokes, the cloud charge structure and discharge processes involved in the formation of LBEs are still unknown.

In this paper, we present an atypical multi-stroke lightning flash recorded at the Säntis Tower. The flash contained 4 strokes, the last 3 of which were normal, while the current waveform associated with the first return stroke of this flash resembled a Gaussian pulse and, as proposed by Chen et al. [8], could be indicative of a process of LBE-type. In order to assess the validity of this hypothesis, we use numerical simulations to reproduce the field signature associated with this current pulse and we compare the obtained parameters of our simulation results with observed field signatures of LBEs in Japan.

The rest of the paper is organized as follows: Section II briefly presents the Säntis Tower experimental setup. Section III contains a description of the observed event. Simulation results are presented in Section IV, along with a comparison with experimental data and discussion. Finally, Section V contains a summary and conclusions.

II. SÄNTIS TOWER INSTRUMENTATION AND OBTAINED DATA

The 124-m tall Säntis Tower, located on the top of Mount Säntis (2502 m Above Sea Level (ASL)), has been instrumented for lightning current measurements since May 2010 [12]. Rogowski coils and multigap B-dot sensors are installed at two different heights, 24 m and 82 m, for measuring the current and its time derivative. The B-dot sensor at the lower height was not present prior to June 29, 2013 (see [13], [14] for more information and recent updates). In this paper, unless otherwise specified, use is made of the combination of the Rogowski coil and the B-dot sensor installed at 82 m to reproduce the current waveform. The Rogowski coil is used to reproduce the low frequency (<100 kHz) part of signal, while the B-dot sensor is used to obtain the high frequency response (>100 kHz). Additional information on the current waveform reconstruction algorithm from the Rogowski coil and the B-dot sensor can be found in [15].

During the period of May 2010 to June 2016, a total of 562 flashes were recorded at the Säntis tower. Out of these, 473 flashes (84%) were classified as negative flashes, 66 (12%) were classified as positive, and 23 (4%) as bipolar. The presence or absence of an initial continuous current was used to classify the recorded events as upward or downward flashes. As expected, more than 99% of the lightning flashes recorded at the Säntis Tower were of the upward type. During the considered period, only three negative and one positive events were classified as downward flashes.

III. DESCRIPTION OF THE EVENT

A. Waveform Characteristics

Among the three negative flashes which were classified as downward based on the absence of the initial continuous current, the one that will be described in this section was a 4-stroke flash recorded on July 15, 2012 at 16:56:36. The overall current waveform of the flash is shown in Figure 1.

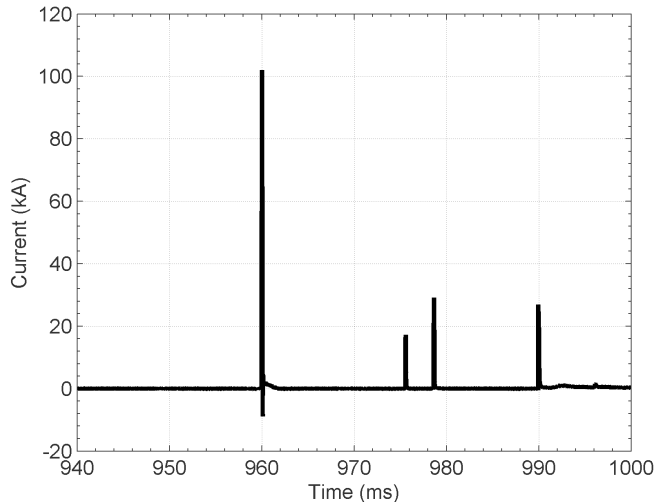


Fig. 1. Overall current waveform of the flash that occurred on 15 July, 2012 at 16:56:36.

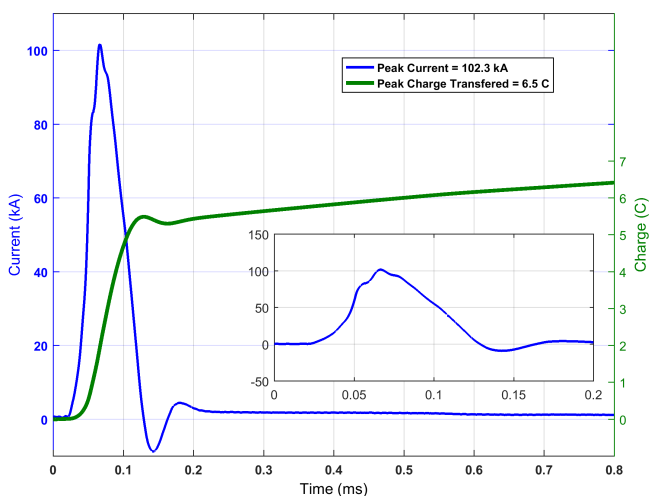


Fig. 2. Measured current (blue) and calculated transferred charge associated with the first return stroke of the flash. An expanded view of the current waveform is shown in the inset.

Note that, throughout the paper, a positive sign for the current is used for negative return strokes, and the atmospheric electricity sign convention (downward directed electric field or electric field change vectors are positive) is adopted for the electric field. The current waveform of the first stroke of this flash, along with its transferred charge, are shown in Figure 2. The waveform appears as a quasi-symmetrical Gaussian-like pulse, which could be associated with an LBE [8]. The peak current of the first stroke is about 102.3 kA and the 10-90% risetime (with respect to the maximum peak) is 28.4 μ s. It is worth mentioning that the 10-90% (with respect to the first peak) risetime is about 20.7 μ s. The initial half-cycle of the

current waveform is followed by an opposite polarity overshoot with a peak of 8.5 kA. The pulse width of the negative half-cycle is 33.7 μ s. Note that the observed overshoot cannot be due to a wave reflection from the tower base, since its occurrence time is much longer than the round-trip time of the wave along the tower (0.55 μ s). Note also that the opposite overshoot is not an artifact of the Rogowski coil for the following reasons: First, the used coils have an air core so there is no saturation effects to be expected. Second, to exclude the possibility of the specific sensor used at 82 m being defective, we compared with measured waveforms from our second, independent Rogowski coil installed at a different height and both measurements are consistent. Third, we have measured strokes with similar peak current amplitudes with no opposite polarity overshoot in the past. Finally, even though the current waveform cannot be faithfully reproduced from the B-dot sensor only (due to the limited low-frequency response of that sensor), the waveform from it exhibits the same overshoot.

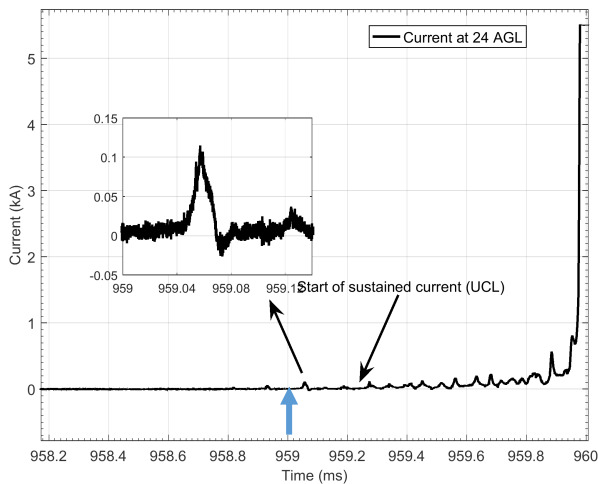


Fig. 3. Expanded view of the initial portion of the current measured at 24 m above ground. The start of sustained upward positive leader current is marked with an arrow. One of the precursor current pulses is shown in the figure inset. The blue arrow indicates the time of occurrence of the positive stroke.

The total charge transferred to ground in 0.8 ms is 6.5 C, which is not far from the 4.5 C median impulse charge reported by *Berger et al.* for first strokes in negative lightning [16]. The current waveform characteristics of this stroke are summarized in Table 1.

Figure 3 shows the recorded current waveform at a height of 24 m along the tower (with better signal to noise ratio compared to the recorded signal at 82 m) in which the start of the sustained (continuously rising) current marked with an arrow, is presumably associated with the start of an upward connecting leader (UCL). Current pulses occurring prior to the start of UCL are referred to as precursor pulses. Similar pulsations have been observed by Biagi et al. [17] in rocket-triggered lightning. Viscaro et al. [18] argued that both the pulses of positive UCL and the preceding precursor pulses are induced by the approaching negative leader. The observed features of the recorded current waveform suggest the involvement of both, a downward and an upward leader in the formation of LBEs.

The first stroke was followed by three other negative strokes

TABLE I
WAVEFORM PARAMETERS OF THE FIRST STROKE OF THE FLASH

Parameter	Value
Initial Half-Cycle Pulse Peak Value (kA)	102.3
Total Transferred Charge (C)	6.5
10-90% Rise Time (μ s)	28.4
Initial Half-Cycle Pulse Width (μ s)	53.7
Negative Half-Cycle Pulse width (μ s)	33.7
Opposite Polarity Overshoot Peak (kA)	-8.5

with peak current values of 17.2, 29.0 and 26.8 kA. Their current waveforms were somewhat similar to that of the first return stroke, but, unlike the first stroke waveform, they started with a faster rising portion with superimposed oscillations and did not exhibit an opposite polarity overshoot. Figure 4 presents expanded views of the current waveforms associated with the second, third, and fourth strokes of this flash. Note that these waveforms are different from those in typical subsequent return strokes in downward flashes, as they include fast oscillations in the rising portion and long time to overall peak of 30 to 40 μ s compared to 0.3-0.6 μ s in typical subsequent return stroke in downward flashes [19]. The oscillations are associated with the transient process in the tower.

Note also that the presence of the tower causes multiple reflections that are only discernible if the tower is electrically long or, equivalently, if the risetime of the current waveform is shorter than the round-trip time along the tower. This is the case for the three subsequent return strokes of this flash. On the other hand, the transient behavior is not visible in the first, slower return stroke current waveform.

In this paper, we will concentrate on the analysis of the first return stroke.

B. Correlation with the Data Provided by the EUCLID Lightning Location System

The flash observed at the Sântis Tower on July 15, 2012 at 16:56:36 was detected by the European Cooperation for Lightning Detection (EUCLID) network [20], [21]. The EUCLID data revealed that this flash was preceded by a positive stroke which occurred 1 ms before the start of the first stroke measured on the tower. The positive stroke was located by EUCLID 0.8 km away from the tower. The peak current value of this stroke was estimated to be 30.1 kA. **It should be noted that there is a chance that EUCLID may misclassified an in-cloud discharge as the positive stroke.**

Figure 5 shows the location of each stroke estimated by EUCLID. It should be noted that only 3 out of 4 strokes of this flash were detected by EUCLID. The third stroke of the flash was missed by EUCLID, even though it had the second highest peak current amplitude.

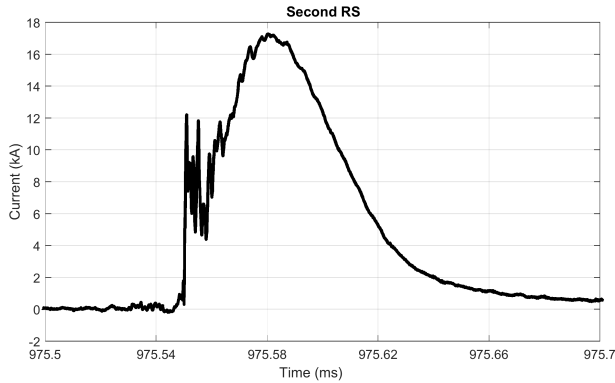
Table 2 presents a comparison between the directly-measured peak currents at the Sântis Tower and the peak current estimates provided by EUCLID.

It can be seen from the table that the EUCLID network systematically overestimated the peak currents. This overestimation can be attributed to the enhancement of the radiated fields due to the propagation along the mountainous terrain [22], [23]. The proximity of the positive stroke in time

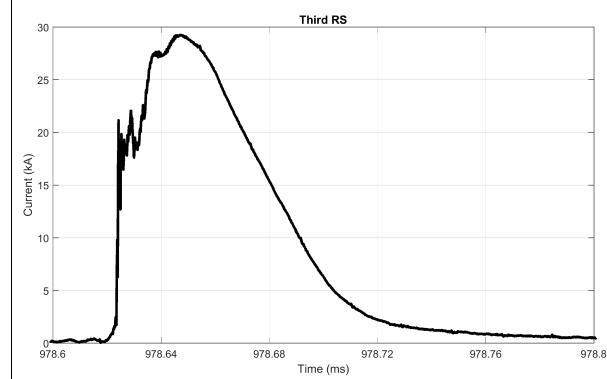
TABLE II
EUCLID PEAK CURRENT ESTIMATES VERSUS PEAK CURRENTS DIRECTLY MEASURED AT THE SÄNTIS TOWER FOR THE RETURN STROKES OF THE FLASH THAT OCCURRED ON JULY 15, 2012 AT 16:56:36.

Stroke Order	Directly measured peak current (kA)	Peak current reported by EUCLID (kA)
1	102.3	126.7
2	17.2	22.9
3	29.0	Not Detected
4	26.8	42.3

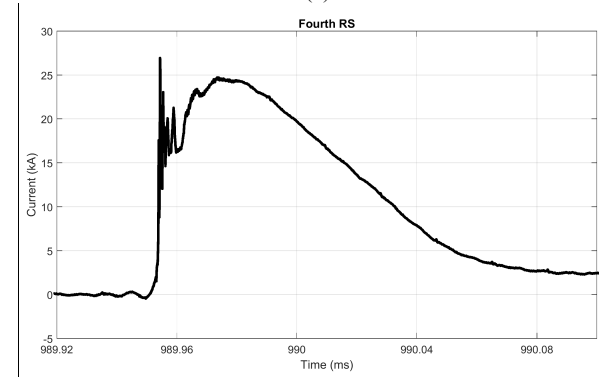
(1 ms) and in space (0.8 km) to the first LBE-like stroke of the flash suggests that this positive stroke might have been involved in the formation process of the tower flash.



(a)



(b)



(c)

Fig. 4. Measured current waveforms associated with three return strokes following the LBE-like stroke of the flash.

TABLE III
PARAMETERS OF DOUBLE HEIDLER FUNCTION WHICH HAS BEEN USED TO REPRESENT THE MEASURED CURRENT WAVEFORM OF LBE-LIKE STROKE.

Parameters (Unit)	I_{01} (kA)	τ_{11} (μ s)	τ_{12} (μ s)	n_1	I_{02} (kA)	τ_{21} (μ s)	τ_{22} (μ s)	n_2
Value	106.7	53	66	8.0	-54.2	122	42	13

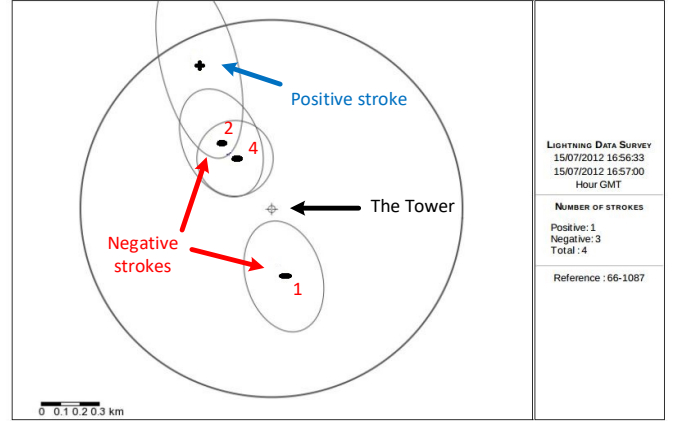


Fig. 5. Detailed locations of strokes reported by EUCLID. The positive stroke occurred 1 ms before the first negative stroke of the flash terminated on the tower. The Sântis Tower location is shown by cross at the center of the figure. The down circle is centered at the Sântis Tower and its radius is 1 km. The positive stroke is shown by a “+” sign and the negative strokes by “-”.

C. Height of the -10°C isotherm

Negative charges are typically located at altitudes corresponding to a temperature range of -10 to -25°C [24]. Azadifar et al. [25] used the Advanced Research Weather Research and Forecast model (WRF-ARW) [26] to evaluate the height of the -10°C isotherm associated with 37 lightning events that occurred at the Sântis Tower (see [25] for more information on the performed WRF-ARW numerical simulations). The considered dataset included 3 downward negative flashes, one of which being the flash analyzed in this work. The dataset also included 28 negative upward flashes and 6 positive upward ones. The derived height of the -10°C isotherm for the flash considered in this paper was 3.9 km ASL. The -10°C isotherm heights for the other two downward negative flashes were 4.2 km and 5 km ASL, respectively. On the other hand, the -10°C ASL altitudes for the upward negative flashes ranged from about 1.9 km to 5.5 km, with a considerable number of flashes having -10°C heights lower than 3 km.

IV. MODELING, NUMERICAL SIMULATION AND COMPARISON WITH EXPERIMENTAL OBSERVATIONS

In this section, we present simulation results for the electric field waveform of the first stroke of the flash discussed in Section III. Two available models describing the charge transfer to ground are used, one of them assuming a return stroke-like process, and the other assuming an M-component-like process.

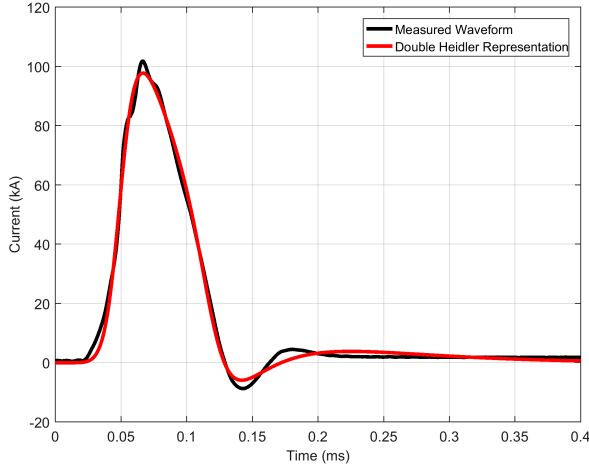


Fig. 6. Double Heidler representation of measured current waveform shown in red.

In order to simplify the process of numerical simulations, the measured current was represented using the sum of two Heidler's functions:

$$i(0,t) = \frac{I_{01}}{\eta_1} \frac{(t/\tau_{11})^{\eta_1}}{[(t/\tau_{11})^{\eta_1} + 1]} e^{-t/\tau_{12}} + \frac{I_{02}}{\eta_2} \frac{(t/\tau_{21})^{\eta_2}}{[(t/\tau_{21})^{\eta_2} + 1]} e^{-t/\tau_{22}} \quad (1)$$

Figure 6 presents the measured current and its analytical representation using two Heidler's functions. The parameters of the Heidler's functions are given in Table 3. Once the distribution of the current along the channel is determined by the charge transfer model, the vertical electric field is computed by integrating along the channel the following expression [27]:

$$dE_z(r,z,z',t) = \frac{dz'}{2\pi\epsilon_0} \left[\frac{2(z-z')^2 - r^2}{R^5} \int_{R/c}^t i(z',\tau - R/c) d\tau + \frac{2(z-z')^2 - r^2}{cR^4} i(z',\tau - R/c) - \frac{r^2}{c^2R^3} \frac{\partial i(z',\tau - R/c)}{\partial t} \right] \quad (2)$$

in which r and z are the cylindrical coordinates of the observation point, R is the distance between each current element along the channel and the observation point ($R = \sqrt{r^2 + (z-z')^2}$), $i(z',t)$ is the element of current along the channel, c is the speed of light, and ϵ_0 is the permittivity of free space. It should be noted that a perfectly-conducting flat ground was assumed and the presence of the tower was ignored.

A. Return Stroke Mode of Charge Transfer

It has been suggested in [8] that both a return stroke-like or an M-component-like charge transfer process might be associated with LBEs. The return stroke mode of charge transfer for the LBE was simulated adopting the MTL model [28], [29]. According to this model, the current distribution along the channel can be expressed as:

$$i(z',t) = \exp(-z'/\lambda) \times i_0(t - z'/v_{RS}) \times u(t - z'/v_{RS}) \quad (3)$$

in which v_{RS} is the return stroke speed and λ is the attenuation constant.

The height of the lightning channel was assumed to be 2 km (consistent with the height of the 10°C isotherm and the mountain height), the current attenuation constant λ was set to 1 km and the return-stroke speed was assumed to be 1.5×10^8 m/s.

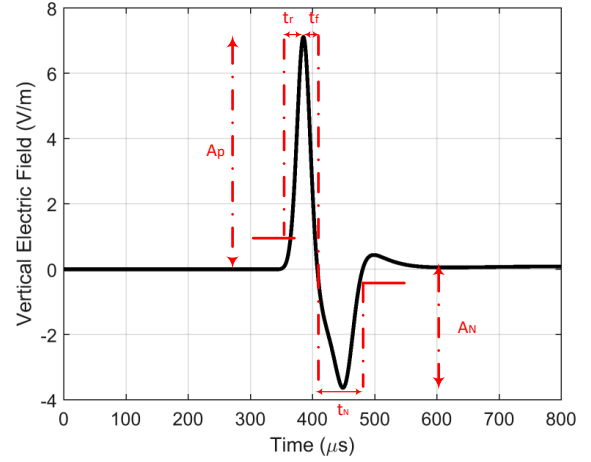


Fig. 7. Vertical electric field at 100 km from the lightning channel associated with the first stroke current of the considered stroke (Fig. 2), computed using the MTL return-stroke model. The height of the channel was assumed to be 2 km, the attenuation constant of the MTL model was set to 1 km, and the return stroke speed was assumed to be 1.5×10^8 m/s.

Figure 7 shows the vertical electric field at a distance of 100 km from the channel. It is clear from Figure 7 that the field waveform shows a bipolar signature similar to LBEs observed in winter thunderstorms in Japan [9], suggesting that a return stroke-like process might be involved in the formation of LBEs.

Figure 8 presents a sensitivity analysis of the field waveform as a function of the return stroke speed (Figure 8a) and the MTL current attenuation constant λ (Figure 8b). It can be seen that an increase in the return stroke speed (Figure 8a) results in a narrower field waveform. Furthermore, an increase in the return stroke speed and in the current attenuation constant results in an increase in the field peaks of both initial half-cycle and opposite polarity overshoot. It is worth mentioning that, based on simulation results (not presented here), the use of the TL model results in a very similar field waveshape, but a larger field peak, compared to the MTL model.

B. M-component Mode of Charge Transfer

Ishii and Saito [2] suggested that LBEs can be initiated by a long upward connecting leader which attaches to a horizontal channel section at a high altitude. They used the Numerical Electromagnetics Code (NEC) to calculate the vertical electric field associated with the horizontal and vertical sections of the channel. The downward progression of the wave in the vertical section of the channel and its reflection from the ground are similar to the 2-wave model for the M-component mode of charge transfer proposed in [30].

We used the guided wave mechanism proposed by Rakov et al. [31] to describe the current distribution along the channel associated with LBEs. As with the return stroke mode of charge transfer simulations presented in Section IV.A, the presence of the tower was neglected in the calculations. Equation 4 presents the expressions for the current distribution along the channel according to Rakov et al.'s guided wave model:

$$i(z,t) = \begin{cases} i(H,t - (H-z)/v_M) & t < H/v_M \\ i(H,t - (H-z)/v_M) + i(H,t - (H+z)/v_M) & t \geq H/v_M \end{cases} \quad (4)$$

in which H is the junction height and v_M is the current wave velocity.

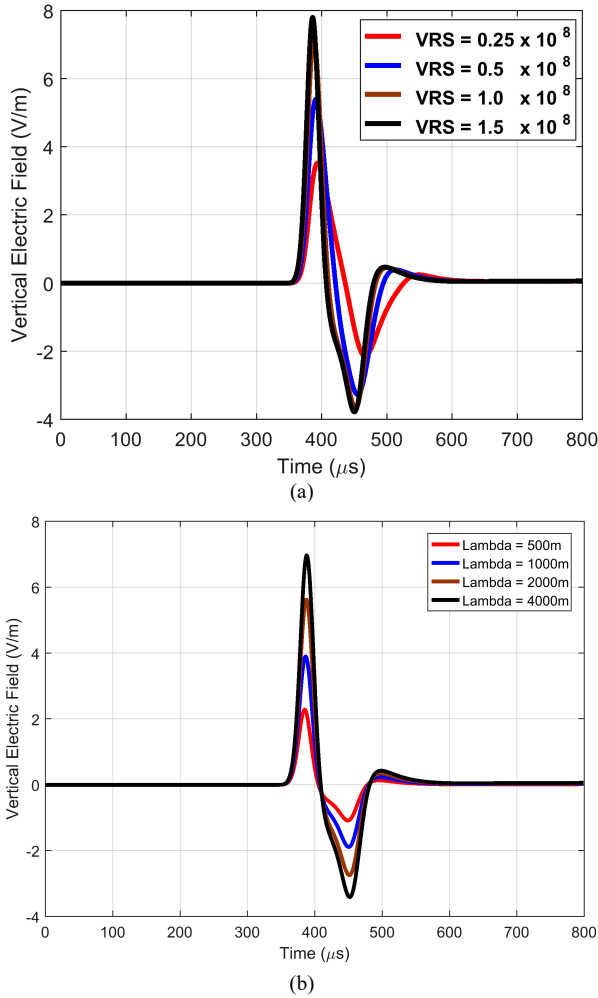


Fig. 8. Vertical electric field at 100 km from the lightning channel associated with the first stroke current of the considered flash (Fig. 2), computed using the MTLT return-stroke model. The height of the channel was assumed to be 2 km. a) The current attenuation constant of the MTLT model was set to 2 km and variation as a function of the return stroke speed is shown. b) Variation as a function of the current attenuation constant. The return stroke speed was set to 1.5×10^8 m/s.

Figure 9 presents vertical electric field waveforms calculated at a distance of 100 km from the channel, for different values of the current wave progression speed (Figure. 9a) and assuming different initiation heights (Figure. 9b). Clearly, the field waveforms become narrower as the velocity of progression increase (Figure 9a). It can be seen that both the wave propagation velocity and the initiation height affect considerably the radiated field. Increasing the speed of the wave results in an increase of both positive and negative field peaks, and a decrease in the initial (positive) half-cycle width (Figure 9a). A higher initiation height also results in higher field peaks of both polarities, and an increase in the width of the positive half-cycle (Figure 9b).

TABLE IV
FIELD WAVEFORM CHARACTERISTICS OF LBES OBSERVED IN JAPAN (ADAPTED FROM WU ET AL. [9])

Parameter	Min	Max	Median
Initial pulse width (μ s)	4	32	15
Ratio of rise to fall time	0.4	4.8	1.4
Ratio of positive to negative pulse width	0.4	2	1.1
Ratio of positive to negative pulse peak	0.4	2.4	1.1

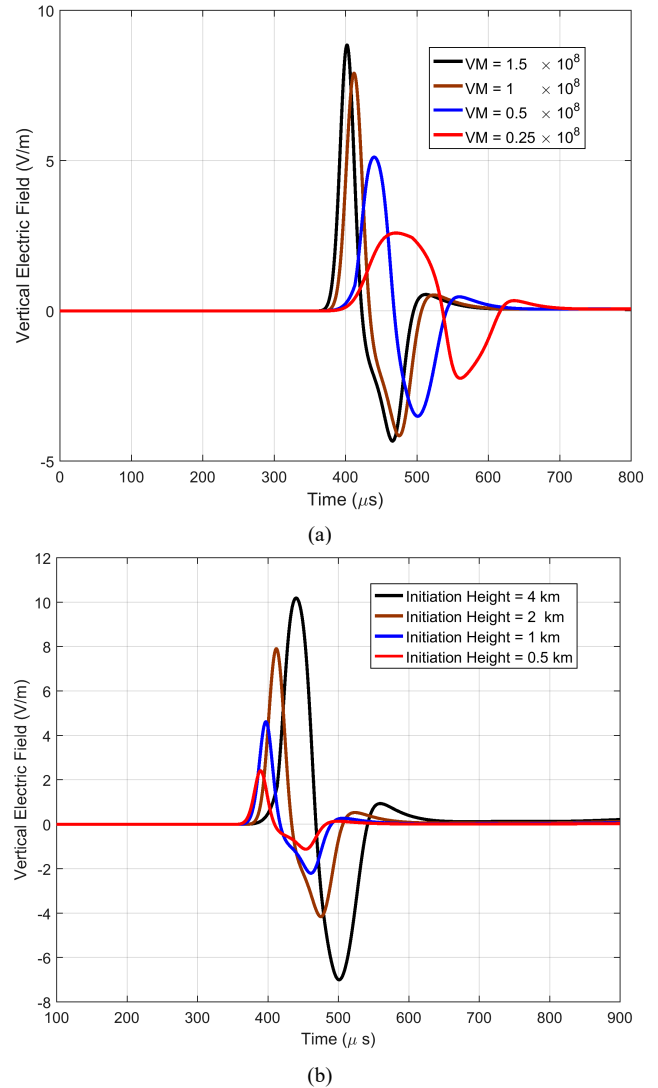


Fig. 9. Vertical electric field at 100 km from the lightning channel associated with the first stroke current of the considered flash (Fig. 2), computed using the guided-wave M-component model of Rakov et al. a) Variation as a function of the return stroke speed (Height = 2 km). b) Variation as a function of the junction height ($v_M = 1 \times 10^8$ m/s).

C. Comparison with LBE Observations

As seen in Figures 8 and 9, the field waveforms calculated using the two models are quite similar. They exhibit the bipolar signature typical of LBES observed in winter storms in Japan. Figure 10 shows an example of observed electric field of LBES in Japan at distance of 236 km (adapted from [9]). Table 4

presents a summary of the parameters of the LBE field waveforms observed in Japan by Wu et al. [9]. It can be seen that, although the ratio of positive to negative pulse peak varies from 0.4 to 2.4 and the ratio of the positive to negative pulse durations varies from 0.4 to 2, both median values are close to 1.

Both the return stroke and M-component models contain adjustable parameters which can affect the resulting field waveform. A sensitivity analysis to assess the effect of the variation of the model parameters on the field salient parameters of the waveform will be presented in the next two subsections.

- The considered parameters for the analysis (see Figure 7) are:
- the initial half-cycle width, defined as the sum of the rise and fall times, t_r+t_f ,
 - the ratio of rise to fall times, t_r/t_f ,
 - the ratio of positive to negative half-cycle widths, $(t_r+t_f)/t_N$,
 - the ratio of the positive to negative field peaks, A_P/A_N ,

where t_r is the time interval between 10% and 100% of the first half-cycle and t_f is the time interval between the peak of the positive half-cycle and the peak of the negative half cycle.

1) Sensitivity Analysis with Respect to the Parameters of the Return-stroke Model

Figure 11 shows the sensitivity of model predictions to variation in two adjustable parameters of the MTL model, namely the return stroke speed v_{RS} and the current attenuation

constant λ . It can be observed that by increasing the value of the return stroke speed, regardless of the attenuation constant, all the considered parameters, except for the positive half-cycle width, are within the range of those in the field observations by Wu et al. in Japan (see Table 4). With increasing the return stroke speed, the positive half-cycle width would tend to a value of about 40 μs , which is somewhat higher than the maximum value of 32 μs reported by Wu et al. [2014]. The discussion presented in the Appendix shows that the parameters of the radiated electric fields tend to those of the current time derivative, with increasing return-stroke speed.

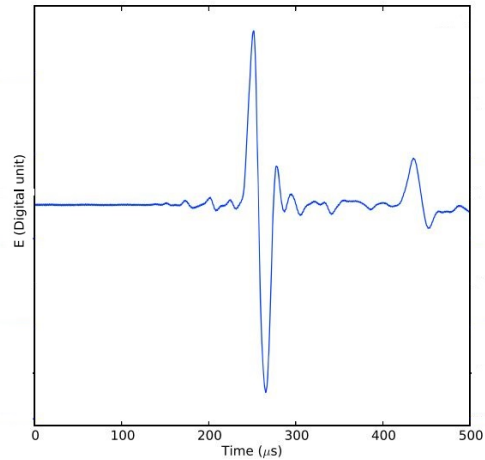


Fig. 10. An example of LBE event observed in Japan (Adapted from [9]).

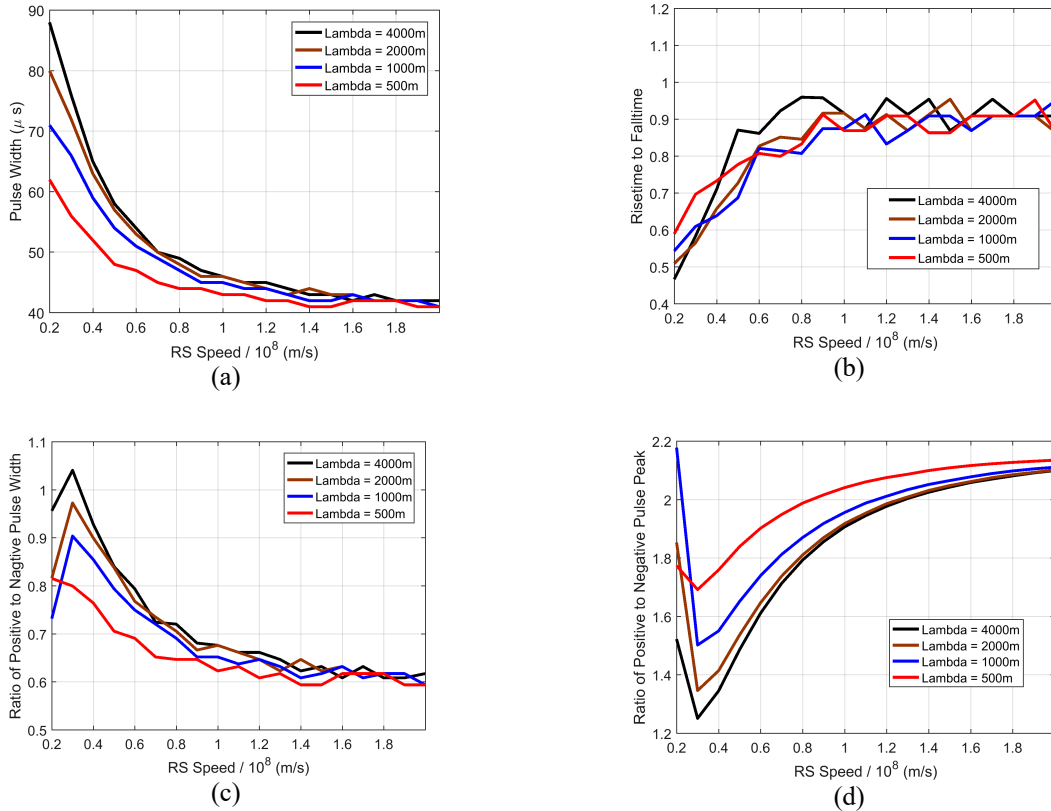


Fig. 11. Sensitivity analysis of the salient parameters of the LBE radiated field at 100 km, assuming a return stroke mode of charge transfer. The height of channel is set to 2 km. a) Positive half-cycle width, b) ratio of rise to fall times, c) ratio of positive to negative half-cycle widths, d) ratio of the positive to negative field peaks.

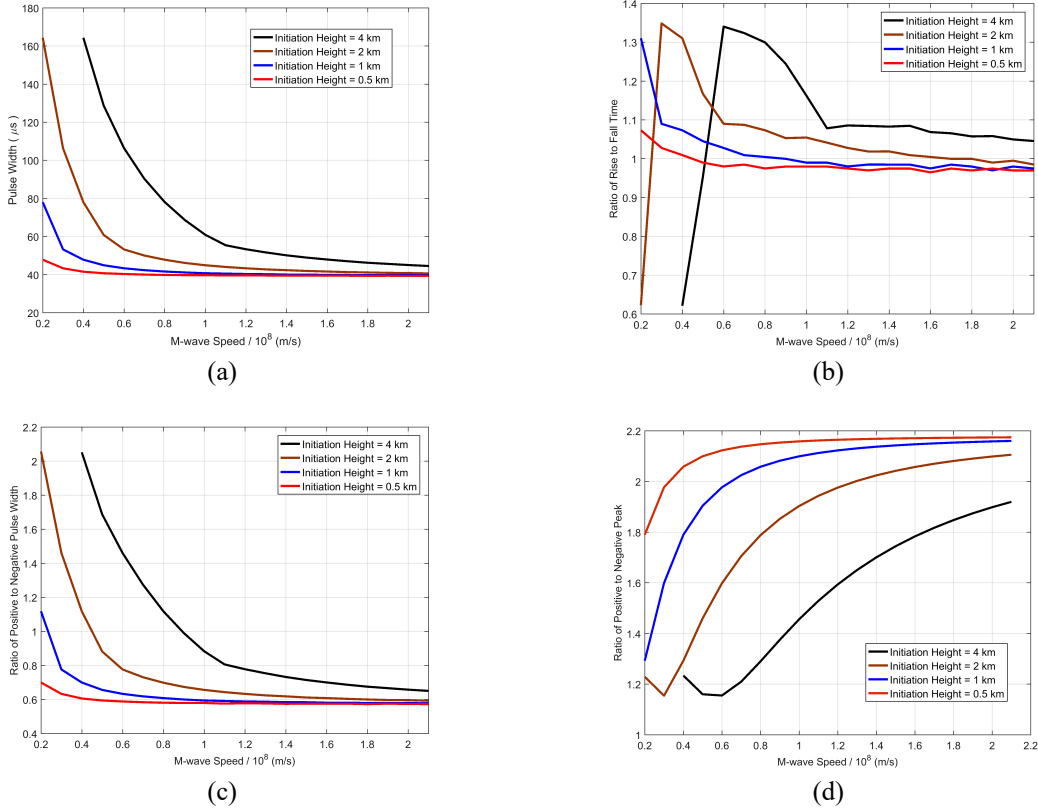


Fig. 12. Sensitivity of M-component model predictions (salient parameters of the LBE radiated field at 100 km) to the variation of V_M and H . a) Positive half-cycle width, b) ratio of rise to fall times, c) ratio of positive to negative half-cycle widths, d) ratio of the positive to negative field peaks.

2) Sensitivity Analysis with Respect to the Parameters of the M-component Model

Figure 12 shows the sensitivity of model predictions to variations in adjustable parameters of the M-component model. In this case, the adjustable parameters are the initiation height (H) and the current wave speed (v_M). It can be seen that, except for the positive half-cycle width, for which the computed values are again larger than the maximum observed value, the ranges of observed values can be reproduced by adjusting the parameters of the model. It is interesting to observe that, similar to the RS model, the positive half-cycle width tends to a value of about 40 μs , which corresponds to the width of the current derivative waveform (see Appendix).

V. SUMMARY AND CONCLUSIONS

We presented a 4-stroke downward negative lightning flash recorded at the Sântis Tower that occurred on July 15, 2012. The current waveform associated with the first return stroke of this flash resembles a Gaussian pulse which, according to [4], could be indicative of an LBE-type event.

We also presented simulation results for the radiated electric fields considering two different models for the LBE and found that the simulated waveforms for both models have characteristics that agree fairly well with the experimentally observed characteristics of radiated fields associated with LBEs, except for the initial (positive) half-cycle width, which

was somewhat larger than the maximum experimentally observed value.

APPENDIX

As seen in Table 1, the current waveform of the LBE-like process presented in this paper is characterized by a relatively slow risetime of 28.4 μs , which is considerably longer than the risetime of normal return strokes. The long risetime indicates that the frequency spectrum of the LBE current waveform contains more lower frequencies compared to return strokes. At lower frequencies, the length of the channel that carries the LBE current can be considered as electrically short, especially for higher current wave speeds. As a result, the higher the propagation speed, the more the channel will look like a Hertzian dipole and, at large distances, the radiation field will be proportional to the derivative of the current, for which we can write:

$$E_z^{far}(r, t) = \frac{Z_0 l}{2\pi r c} \left(\frac{di(t)}{dt} \right) \quad (\text{A1})$$

where l is the length of the channel, c is the speed of light, $Z_0=120\pi$ is the intrinsic impedance of the free space, and r is the distance to the observation point.

To illustrate the above point, we have plotted the derivative of the measured current waveform in Figure A1. The parameters of the current derivative waveform are given on the figure. With reference to Figures 11 and 12, we can see that, indeed, as the speed of the current wave increases, the values of

the parameters of the field waveforms tend to those of the current derivative. For instance, the initial pulse width of the calculated field tends to 37 μs as the speed increases to 1.5×10^8 m/s (see Figure 8a). This value is indeed very similar to the width of the initial half-cycle of the current derivative waveform (see Figure A1).

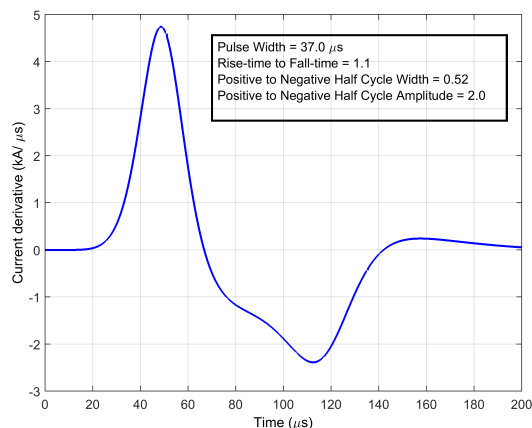


Fig. A1. Current derivative waveform of LBE event recorded at Säntis Tower.

ACKNOWLEDGMENT

Financial supports from the Swiss National Science Foundation (Projects No. 200021_147058 and 200020_175594) and the European Union's Horizon 2020 research and innovation program (grant agreement. No 737033-LLR) are acknowledged.

REFERENCES

- [1] M. Ishii, M. Saito, F. Fujii, M. Matsui, and N. Itamoto, "High-current lightning discharges in winter," *Electr. Eng. Japan*, vol. 170, no. 1, pp. 8–15, Jan. 2010.
- [2] M. Ishii and M. Saito, "Lightning Electric Field Characteristics Associated With Transmission-Line Faults in Winter," *IEEE Trans. Electromagn. Compat.*, vol. 51, no. 3, pp. 459–465, Aug. 2009.
- [3] C. D. Weidman and E. P. Krider, "The fine structure of lightning return stroke wave forms," *J. Geophys. Res.*, vol. 83, no. C12, p. 6239, 1978.
- [4] M. Saito, M. Ishii, F. Fujii, and M. Matsui, "Seasonal Variation of Frequency of High Current Lightning Discharges Observed by JLDN," *IEEE Trans. Power Energy*, vol. 132, pp. 536–541, 2012.
- [5] M. Saito and M. Ishii, "Reproduction of Electric Field Waveforms Associated with GC strokes Hitting Wind turbines," in *4th International Symposium on Winter Lightning*, 2017.
- [6] H. Kaneko, N. Itamoto, and K. Shinjo, "Application of TL Model for Estimation of Current Waveform of Winter Lightning," in *4th International Symposium on Winter Lightning*, 2017.
- [7] A. Nag and V. A. Rakov, "Compact intracloud lightning discharges: I. Mechanism of electromagnetic radiation and modeling," *J. Geophys. Res. Atmos.*, vol. 115, no. 20, pp. 1–20, 2010.
- [8] L. Chen, Q. Zhang, W. Hou, and Y. Tao, "On the field-to-current conversion factors for large bipolar lightning discharge events in winter thunderstorms in Japan," *J. Geophys. Res. Atmos.*, vol. 120, no. 14, p. 2015JD023344, 2015.
- [9] T. Wu, S. Yoshida, T. Ushio, Z. Kawasaki, Y. Takayanagi, and D. Wang, "Large bipolar lightning discharge events in winter thunderstorms in Japan," *J. Geophys. Res. Atmos.*, vol. 119, no. 2, pp. 555–566, Jan. 2014.
- [10] Y. Zhu, V. A. Rakov, and M. D. Tran, "Optical and electric field signatures of lightning interaction with a 257-m tall tower in Florida," *Electr. Power Syst. Res.*, vol. 153, pp. 128–137, Dec. 2017.
- [11] Y. Zhu, V. A. Rakov, M. D. Tran, W. Lyu, and D. D. Micu, "A Modeling Study of Narrow Electric Field Signatures Produced by Lightning Strikes to Tall Towers," *J. Geophys. Res. Atmos.*, vol. 123, no. 18, p. 10,260–10,277, Sep. 2018.
- [12] C. Romero, M. Paolone, M. Rubinstein, F. Rachidi, A. Rubinstein, G. Diendorfer, W. Schulz, B. Daout, A. Kälin, and P. Zwiackker, "A system for the measurements of lightning currents at the Säntis Tower," *Electr. Power Syst. Res.*, vol. 82, no. 1, pp. 34–43, 2012.
- [13] M. Azadifar, M. Paolone, D. Pavanello, C. Romero, F. Rachidi, and M. Rubinstein, "An update on the instrumentation of the Säntis Tower in Switzerland for lightning current measurements and obtained results," in *CIGRE International Colloquium on Lightning and Power Systems*, 2014.
- [14] C. Romero, M. Paolone, M. Rubinstein, F. Rachidi, A. Rubinstein, G. Diendorfer, W. Schulz, B. Daout, A. Kälin, and P. Zwiackker, "A system for the measurements of lightning currents at the Säntis Tower," *Electr. Power Syst. Res.*, vol. 82, no. 1, pp. 34–43, 2012.
- [15] C. Romero, F. Rachidi, A. Paolone, and M. Rubinstein, "Statistical Distributions of Lightning Current Parameters Based on the Data Collected at the Säntis Tower in 2010 and 2011," *IEEE Trans. Power Deliv.*, vol. 28, no. 3, pp. 1804–1812, 2013.
- [16] K. Berger, R. B. Anderson, and H. Kroninger, "Parameters of lightning flashes," *Electra*, vol. 41, pp. 23–37, 1975.
- [17] C. J. Biagi, M. A. Uman, J. D. Hill, D. M. Jordan, V. A. Rakov, and J. Dwyer, "Observations of stepping mechanisms in a rocket-and-wire triggered lightning flash," *J. Geophys. Res. Atmos.*, vol. 115, no. 23, pp. 2–7, 2010.
- [18] S. Visacro, M. Guimaraes, and M. H. Murta Vale, "Features of Upward Positive Leaders Initiated From Towers in Natural Cloud-to-Ground Lightning Based on Simultaneous High-Speed Videos, Measured Currents, and Electric Fields," *J. Geophys. Res. Atmos.*, vol. 122, no. 23, p. 12,786–12,800, Dec. 2017.
- [19] V. A. Rakov and M. A. Uman, *Lightning Physics and Effects*. Cambridge University Press, 2003.
- [20] W. Schulz, G. Diendorfer, S. Pedebay, and D. R. Poelman, "The European lightning location system EUCLID – Part 1: Performance analysis and validation," *Nat. Hazards Earth Syst. Sci.*, vol. 16, no. 2, pp. 595–605, Mar. 2016.
- [21] D. R. Poelman, W. Schulz, G. Diendorfer, and M. Bernardi, "The European lightning location system EUCLID – Part 2: Observations," *Nat. Hazards Earth Syst. Sci.*, vol. 16, pp. 607–616, 2016.
- [22] D. Li, M. Azadifar, F. Rachidi, M. Rubinstein, M. Paolone, D. Pavanello, S. Metz, Q. Zhang, and Z. Wang, "On Lightning Electromagnetic Field Propagation Along an Irregular Terrain," *IEEE Trans. Electromagn. Compat.*, vol. 58, no. 1, pp. 161–171, Feb. 2016.
- [23] A. Smorgonskiy, A. Tajalli, M. Rubinstein, G. Diendorfer, and H. Pichler, "An analysis of the initiation of upward flashes from tall towers with particular reference to Gaisberg and Säntis Towers," *J. Atmos. Solar-Terrestrial Phys.*, vol. 136, pp. 46–51, Dec. 2015.
- [24] P. R. Krehbiel, "The electrical structure of thunderstorms in The Earth's Electrical Environment," in *Earth's Electrical Environment*, Washington, D.C: National Acad. Press, 1986, pp. 90–113.
- [25] M. Azadifar, M. Lagasio, E. Fiori, F. Rachidi, M. Rubinstein, and R. Procopio, "Occurrence of Downward and Upward Flashes at the Säntis Tower: Relationship with -10 degrees C Temperature Altitude," in *European Electromagnetics International Symposium EUROEM*, 2016.
- [26] C. Skamarock, B. Klemp, J. Dudhia, O. Gill, M. Barker, W. Wang, and G. Powers, "A Description of the Advanced Research WRF Version 2," 2005.
- [27] M. Rubinstein and M. A. Uman, "Methods for calculating the electromagnetic fields from a known source distribution: Application to lightning," *IEEE Trans. Electromagn. Compat.*, vol. 31, no. 2, pp. 183–189, 1989.
- [28] C. A. Nucci, C. Mazzetti, F. Rachidi, and M. Ianoz, "On lightning return stroke models for LEMP calculations," in *19th International Conference on Lightning Protection*, 1988.
- [29] F. Rachidi and C. A. Nucci, "On the Master, Uman, Lin, Standler and the Modified Transmission Line Lightning return stroke current models," *J. Geophys. Res.*, vol. 95, no. D12, p. 20389, 1990.
- [30] V. A. Rakov, R. Thottappillil, M. A. Uman, and P. P. Barker, "Mechanism of the lightning M component," *J. Geophys. Res.*, vol. 100, no. D12, p. 25701, 1995.
- [31] V. A. Rakov, D. E. Crawford, K. J. Rambo, G. H. Schnetzer, M. A.

Uman, and R. Thottappillil, "M-component mode of charge transfer to ground in lightning discharge," *J. Geophys. Res. Atmos.*,

vol. 106, no. D19, pp. 22817–22831, 2001.